Estimation of sheath potentials in front of ASDEX upgrade ICRF antenna with SSWICH asymptotic code

A. Křivská, V. Bobkov, L. Colas, J. Jacquot, D. Milanesio, R. Ochoukov, and ASDEX Upgrade team

Citation: AIP Conference Proceedings **1689**, 050002 (2015); doi: 10.1063/1.4936490
View online: http://dx.doi.org/10.1063/1.4936490
View Table of Contents: http://aip.scitation.org/toc/apc/1689/1
Published by the American Institute of Physics

Estimation of sheath potentials in front of ASDEX Upgrade ICRF antenna with SSWICH asymptotic code

A. Křivská[1, a)], V. Bobkov[2], L. Colas[3], J. Jacquot[2], D. Milanesio[4], R. Ochoukov[2] and ASDEX Upgrade team[2]

[1]*LPP-ERM/KMS, Royal Military Academy, 30 Avenue de la Renaissance B-1000, Brussels, Belgium*
[2]*Max-Planck-Institut für Plasmaphysik, D-85748 Garching, Germany*
[3]*CEA, IRFM, F-13108 Saint-Paul-Lez-Durance, France*
[4]*Politecnico di Torino, Corso Duca degli Abruzzi 24, I-10129 Torino, Italy*

[a)]Corresponding author: alena.krivska@rma.ac.be

Abstract. Multi-megawatt Ion Cyclotron Range of Frequencies (ICRF) heating became problematic in ASDEX Upgrade (AUG) tokamak after coating of ICRF antenna limiters and other plasma facing components by tungsten. Strong impurity influx was indeed produced at levels of injected power markedly lower than in the previous experiments. It is assumed that the impurity production is mainly driven by parallel component of Radio-Frequency (RF) antenna electric near-field $E_{//}$ that is rectified in sheaths. In this contribution we estimate poloidal distribution of sheath Direct Current (DC) potential in front of the ICRF antenna and simulate its relative variations over the parametric scans performed during experiments, trying to reproduce some of the experimental observations. In addition, relative comparison between two types of AUG ICRF antenna configurations, used for experiments in 2014, has been performed. For this purpose we use the Torino Polytechnic Ion Cyclotron Antenna (TOPICA) code and asymptotic version of the Self-consistent Sheaths and Waves for Ion Cyclotron Heating (SSWICH) code. Further, we investigate correlation between amplitudes of the calculated oscillating sheath voltages and the $E_{//}$ fields computed at the lateral side of the antenna box, in relation with a heuristic antenna design strategy at IPP Garching to mitigate RF sheaths.

INTRODUCTION

Multi-megawatt Ion Cyclotron Range of Frequencies (ICRF) heating became problematic in ASDEX Upgrade (AUG) tokamak after coating of ICRF antenna limiters and other plasma facing components by tungsten. Strong impurity influx was indeed produced at levels of injected power markedly lower than in the previous experiments. [1, 2]. It is assumed that the impurity production is mainly driven by Radio-Frequency (RF) antenna electric near-field $E_{//}$, parallel to the confinement magnetic field $\mathbf{B}_0$ of the tokamak [3]. $E_{//}$ field generates oscillations of voltages V_{RF} across thin boundary layers (sheaths) where a line of the confinement magnetic field intercepts a conducting obstacle. In these rectifying RF sheaths, the oscillating V_{RF} cause enhanced Direct Current (DC) plasma potentials V_{DC}. Ions are accelerated along the confinement field lines, hit the obstacle and thus enhance tungsten sputtering and localized heat flux. V_{DC} exceeding 100 V is needed to induce significant tungsten sputtering by incident light impurity and deuterium ions [4]. In this contribution we estimate the poloidal distribution of the potentials V_{DC} in front of two AUG ICRF antenna configurations and simulate its relative variations over the parametric scans performed during experiments, trying to reproduce some of the experimental observations. Further, we investigate correlation between amplitudes of the oscillating voltages V_{RF} and the $E_{//}$ field computed at the lateral side of the antenna box.

DESCRIPTION OF SIMULATION OF THE SHEATH POTENTIALS

For estimation of the poloidal distribution of the sheath potential V_{DC} in front of the ICRF AUG antenna we use the asymptotic version of the Self-consistent Sheaths and Waves for Ion Cyclotron Heating (SSWICH) code [5]. It

Radio Frequency Power in Plasmas
AIP Conf. Proc. 1689, 050002-1–050002-4; doi: 10.1063/1.4936490

was chosen because it is rapid, robust, always provides systematically one solution for each set of input parameters and convergence is guaranteed. It is suitable for relative comparisons of antenna designs and electrical settings. In this code, slow wave propagation in the bounded scrape-off layer (SOL) plasma from a prescribed map of $E_{//}$ field is described self-consistently with DC biasing of the SOL, via non-linear RF and DC sheath boundary conditions at both ends of open magnetic field lines. $E_{//}$ field generates oscillations of voltages V_{RF} across sheaths at both lateral sides of the private SOL. DC plasma potentials are obtained from the rectification of the oscillating RF voltages driving the sheaths. Main disadvantages of the code are related to number of approximations made on the original physical model. Simple 3-dimensional parallelepiped simulation domain with walls normal to the straight magnetic field lines and only slow wave (SW), responsible for excitation of the RF sheaths when the side walls are normal to $\mathbf{B}_0$, were only adopted. Sketch of the simulation domain can be found in [6]. It involves only private SOL between antenna limiters, while most measurements are available in the main SOL [7]. Furthermore, the parallel DC plasma conductivity is taken as infinite while transverse plasma conductivity is neglected in the simplified model of DC plasma biasing. With this choice of parameters, the DC Plasma potential V_{DC} is homogeneous all along the open field lines and depends only on the V_{RF} values at both ends of these field lines. In our simulations, approximations are also made on the antenna and plasma geometry. The real curved antenna structure is represented by a flat model. We consider two types of antenna configurations that were used for experiments in 2014: initial narrow and partly optimized wide antenna configuration. Figures of the antennas and more detailed description of the optimized antenna can be found in [7].

Main input to the SSWICH code - the 2D $E_{//}$ field maps in front of the antenna - are produced by the TOPICA antenna code [8] in absence of sheaths. In TOPICA simulations, the antenna model is placed into a metallic recess facing an inhomogeneous magnetized SOL plasma. We located the plasma edge surface 5 mm above the leading edge of the limiters. In that point we faced difficulties where to place the surface for the $E_{//}$ field map calculation which represents interface between the TOPICA and the SSWICH codes in case of the AUG antenna. After several tests we decided to place this interface only 3.2 mm behind the leading edge of the limiters and 10 mm above the Faraday screen (FS) in the vacuum region in order to include properly the influence of the current density circulation on the limiters. In the simulations, plasma kinetic profiles in L-mode obtained during experiments in 2014 are used as the plasma input parameters. Plasma geometry is assumed slab with temperature and density gradients along minor radius of the tokamak chamber. All the considered plasma scenarios include 3% of hydrogen minority in deuterium with diagonal elements of the cold plasma dielectric tensor [9] $\varepsilon_\perp$ = -25 – -13 and $\varepsilon_{//}$ = -75530 – -40700 at the plasma edge. Magnetic field in plasma center B_T = 1.9 T, 11^0 tilted with respect to the toroidal direction, is taken into account. Simulations are performed for various antenna electrical settings: a) (0 π) phasing, b) (0 160^0) phasing, c) (0 $-\pi/2$) phasing, d) (0 $+\pi/2$) phasing, e) (0 π) phasing with ratio of strap powers 1:4 and f) (0 π) phasing with ratio of strap powers 4:1. The RF field maps are evaluated for operational frequency 30 MHz and normalized to 240 kW of RF power coupled to the target plasma using scattering matrix obtained at the antenna feeders.

Distribution of the sheath potential V_{DC} is calculated starting from a reference plane placed 1 mm above the FS. All the input $E_{//}$ field maps are retro-propagated to this reference plane by applying coefficient $[1+k_p * \delta x_2] / [1+k_p * \delta x_1]$, where the squared SW radial wave vector $k_p^2 = -\varepsilon_{//} (k_0^2 - k_{//}^2/\varepsilon_\perp) + k_y^2$, δx_1 is distance between the electric field surface and the plasma boundary (in this case δx_1 = 8.18 mm) and δx_2 is distance between the plasma boundary and the SSWICH reference plane (in this case δx_2 = 17.18 mm). The simulation domain of the SSWICH asymptotic code is bounded in toroidal and radial direction with respective extensions $L_{//}$ and $L_\perp$. Parallel connection length $L_{//}$ = 0.6506 m is chosen to be equal to size of the antenna box in toroidal direction. Gap of 2 mm is added on each side of the $E_{//}$ field maps to correctly take into account the given boundary condition in the SSWICH code. Radial extension $L_\perp$ = 1.22 cm is chosen to be equal to the radial extension of the antenna side limiters.

SIMULATION RESULTS AND COMPARISON WITH EXPERIMENTS

2D radial/poloidal distributions of the sheath potentials V_{DC} calculated for various electrical settings of the broad limiter antenna are showed in Figure 1. In radial direction, peaked values of the V_{DC} are situated 1-3 mm above the SSWICH reference plane. In poloidal direction, increased values are located around y = 0.45 m in the upper part, around y = -0.45 m in the bottom part and in some cases also around the central part of the antenna. Table 1 presents overview of peaked values of the V_{DC} in the upper and bottom part of both antenna configurations with various electrical settings. The relative comparison shows the peaked values of the V_{DC} lower by factor of 1.3 – 3.9, depending on the antenna electrical setting and poloidal position, for the partly optimized broad limiter antenna. In front of the upper part of the broad limiter antenna, the maximal values of the V_{DC} are estimated for (0 $-\pi/2$) and (0 $+\pi/2$) phasing.

In front of the bottom part of the broad limiter antenna, the maximal values of the V_{DC} are evaluated for (0 +π/2) phasing and (0 π) phasing with ratio of strap powers 1:4.

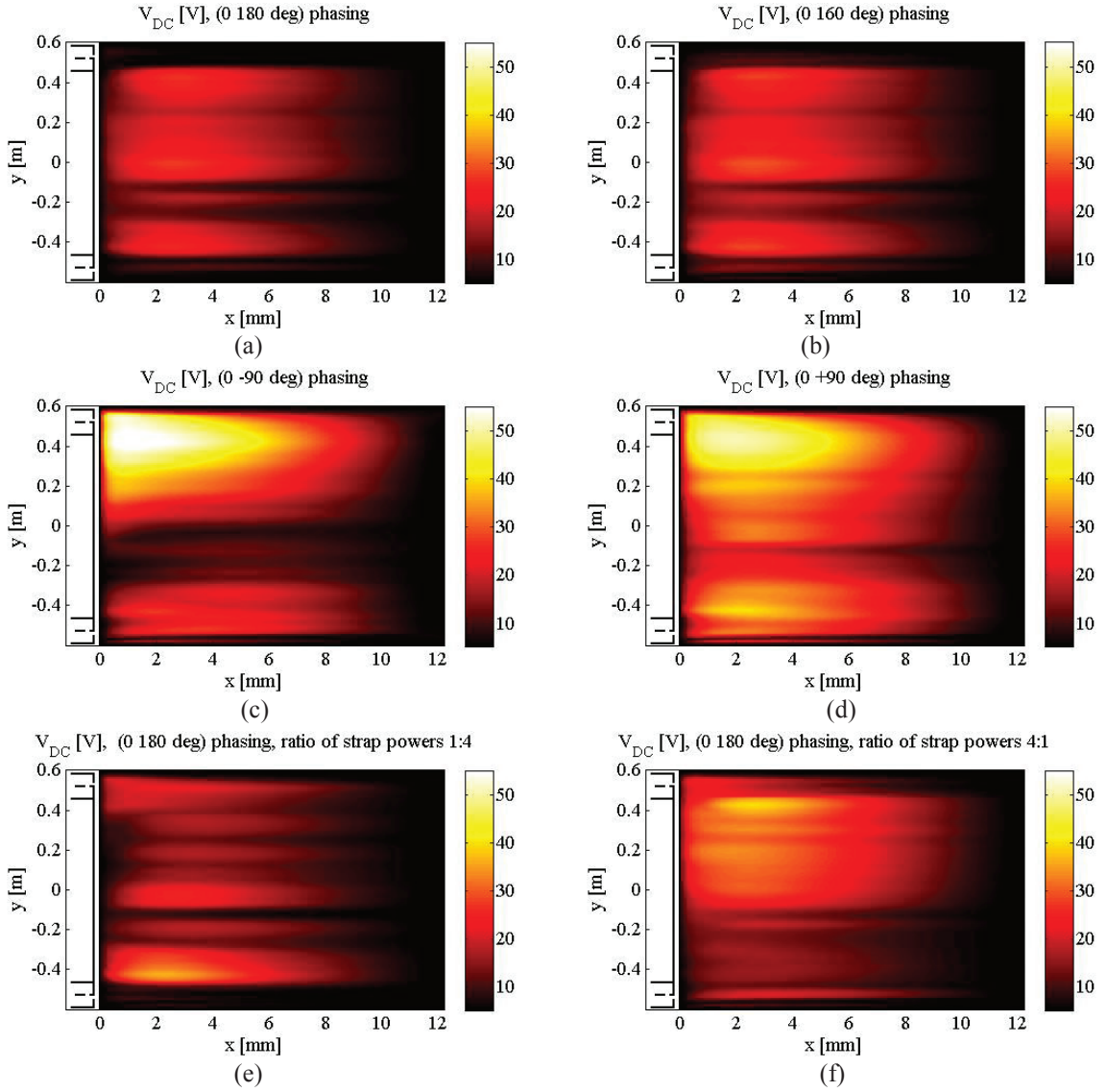

FIGURE 1. 2D radial/poloidal plots of the DC plasma potentials from RF sheath rectification with sketch of the parallelogram-shaped surface where the $E_{//}$ field map is calculated. Each point of the map is representative of 1 open field line. x=0 corresponds to the SSWICH reference plane placed 1 mm above FS while x=12mm is the leading edge of ICRF antenna limiters.

During experimental campaign in 2014, modifications of the SOL plasma were explored in AUG during ICRF heating using a reciprocating retarding field analyzer (RFA) [10]. Combining multiple RFA reciprocations over a scan of q_{95}, 2D poloidal/radial maps of mean parallel ion energies in front of the bottom part of the broad limiter antenna were obtained for the various electrical settings of the magnetically connected antenna. The measurements could not be performed for the upper part of the antenna because it was not magnetically connected to the RFA. The highest mean parallel ion energies, exceeding 160 eV, were measured locally 0-3 mm behind the limiter leading edge around poloidal position y = -0.45 m for (0 +π/2) phasing and (0 π) phasing with ratio of strap powers 1:4. Ion energies remained below 40 eV with a passive antenna. The simulation results for the broad limiter antenna configuration capture qualitatively the relative behavior observed experimentally. On the other hand the absolute values of eV_{DC} are low compared to the measured ion energies and the radial variations do not match exactly. It could be due to the simple simulation domain which corresponds to the private SOL between antenna limiters, while RFAs probe the main SOL

around the active antennas. Furthermore, the simulation results appear to be sensitive to badly known input parameters: the transverse plasma DC conductivity and geometric simulation parameters $L_{//}$ and $L_{\perp}$ [11]. Possible error in the input TOPICA $E_{//}$ field maps could also be the cause.

TABLE 1. Overview of calculated peaked values of the V_{DC} in the upper and bottom part of both antenna configurations with various electrical settings.

Antenna design, settings	Maximal V_{DC} [V] in upper / lower parts
Narrow, (0 π) phasing	55 / 53
Narrow, (0 160^0) phasing	57 / 57
Narrow, (0 -π/2) phasing	71 / 79
Narrow, (0 +π/2) phasing	70 / 84
Narrow, strap powers 1:4	44 / 83
Narrow, strap powers 4:1	157 / 55
Broad, (0 π) phasing	28 / 26
Broad, (0 160^0) phasing	29 / 29
Broad, (0 -π/2) phasing	55 / 28
Broad, (0 +π/2) phasing	52 / 40
Broad, strap powers 1:4	23 / 37
Broad, strap powers 4:1	40 / 22

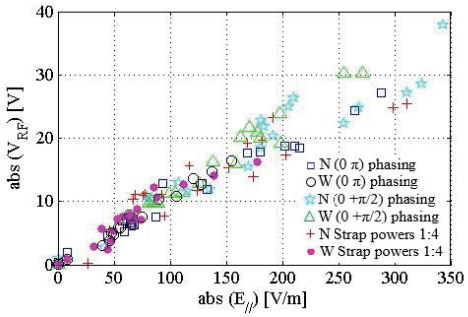

FIGURE 2. Correlations between amplitudes of the potentials V_{RF} and the $E_{//}$ fields at both toroidal edges of the input maps for narrow (N) and wide (W) antenna configurations.

According to the simulations, RF sheaths are mitigated for the broad limiter antenna compared to narrow limiter one. This seems due to dependency of the poloidal distribution of the sheath potentials on the $E_{//}$ fields at the lateral sides of the antenna box that are reduced in case of the broad limiter antenna. More detailed investigations are performed in [6]. Figure 2 shows correlation between amplitudes of the oscillating sheath voltages V_{RF} and the $E_{//}$ fields at both toroidal edges of the input maps for selected antenna settings. The RF sheath voltages are averaged in radial direction and exponential weight function is applied on the $E_{//}$ field maps, with a parallel decay length of 10 cm. The changed electrical settings modify V_{RF} and thus also the V_{DC} voltages. These modifications are correlated with the amplitudes of $E_{//}$ at the lateral sides of the input field maps. The correlation coefficients are in the range of 0.88-0.99 for all the simulated cases. The slope of the line is very similar for the broad and narrow limiter antennas. It depends mainly on plasma parameters.

CONCLUSIONS AND PROSPECTS

First RF-sheath estimates with SSWICH code capture qualitatively the relative variations observed experimentally on AUG. Correlation of V_{RF} with $E_{//}$ averaged over the toroidal sides of the input RF field maps support the strategy of reduction of the $E_{//}$ fields at the lateral sides of the antenna box, followed for the design of the new AUG ICRF 3-strap antenna. [7, 12].

In the next step, simulations with the SSWICH code will be repeated for both AUG ICRF antenna configurations with input $E_{//}$ field maps from the 3D coupling code introduced in [13], to exclude possible errors in the antenna models and in the input $E_{//}$ field maps, and reach better quantitative agreement. Further simulations will study the 3-strap antenna with various electrical settings.

Acknowledgements. This work has been carried out within the framework of the EUROfusion Consortium and has received funding from the Euratom research and training programme 2014-2018 under grant agreement No 633053. The views and opinions expressed herein do not necessarily reflect those of the European Commission. This work was carried out using the HELIOS supercomputer system at Computational Simulation Centre of Inter-national Fusion Energy Research Centre (IFERC-CSC), Aomori, Japan, under the Broader Approach collaboration between Euratom and Japan, implemented by Fusion for Energy and JAEA.

REFERENCES

1. V. Bobkov et al., *JNM* **363–365**, 122-126 (2007).
2. V. Bobkov et al., *JNM* **390–391**, 900-903 (2009).
3. F.W. Perkins, *Nucl. Fus.* **29**, p. 583-592, (1989).
4. V. Bobkov et al., *Nucl. Fus.* **50** 035004, (2010).
5. L. Colas et al., Phys. Plasmas **19** 092505, (2012).
6. L. Colas et al., these proceedings (2015).
7. V. Bobkov et al., *Nucl. Fus.* **53** 093018, (2013).
8. V. Lancellotti et al., *Nucl. Fus.* **46**, S476 (2006).
9. T.H. Stix, "Waves in Plasmas", AIP Press (1992).
10. M. Kočan et al., *Nucl. Fusion* **52** 023016, (2012).
11. J. Jacquot, et al. *Phys. Plasmas* **21**, 061509 (2014).
12. V. Bobkov et al., these proceedings (2015).
13. J. Jacquot et al., these proceedings (2015).